J Therm Anal Calorim (2009) 96:835–840
DOI 10.1007/s10973-009-0052-1

Mesomorphic properties of 5boSOMH from new three rings thiobenzoate series

M. D. Ossowska-Chruściel · A. Rudzki · J. Chruściel

Received: 11 July 2008 / Accepted: 19 May 2009 / Published online: 30 June 2009

Abstract Phase polymorphism of a novel chiral liquid crystalline compound (S)-(+)-4-{4-(4-n-pentylbicyclo[2,2,2] octancarbonylthio)benzoyloxy}benzoate 1-methylheptyl (in short: 5boSOMH) was examined with three complementary methods: Differential Scanning Calorimetry (DSC), Polarized Light Optical Microscopy (POM) and Transmitted Light Intensity (TLI). X-Ray diffraction was used to learn about molecular arrangement in ordered phases. 5boSOMH has two enantiotropic phases: SmB* and SmA*, and exhibits solid phase polymorphism.

Keywords Chiral liquid crystal · Phase polymorphism · SmB* and SmA* phases · Thiobenzoate

Introduction

Thermal behaviour of some liquid crystals esters have been studied recently [1]. Achiral compounds of general formula (Fig. 1), with ester groups (–COO–) as central bridges (X, Y) are monomorphic, nematic-only liquid crystals, regardless of the kind of terminal substituents R and R′ [2– 4].

Replacing the ester bridge X (Fig. 1) at the bicyclooctane ring with a –C–C– bond significantly affects the phase situation. Depending on the kind and the length of the terminal groups (–R, –OR) as well as their location within the molecule, the compounds adopt smectic G (SmG), smectic C (SmC) or nematic (N) mesophases [5–7]; whenever X = –C–C–, Y = –COO–, R = $-C_6H_{13}$ and R′ = $-C_{10}H_{21}$ [5] or X = –C–C–, Y = –OOC–, R = $-C_6H_{13}$ and R′ = $-OC_8H_{17}$, they assume the smectic B (SmB), smectic A (SmA) or nematic phases. However, if the central bridge Y is –C–C–, then the compounds have only one, nematic, liquid crystalline phase [8]. If the terminal substituent R at the bicyclooctane ring is chiral, and if the central bridges are: X = –C–C– and Y = –COO–, and if R′ is either a 1-methylpropyloxy [6, 7] group or 1-methylheptyloxy [5] group, then the compounds have SmB* and cholesteric (Ch) phases. The structures of the central bridges as well as their location in a three-ring molecule are therefore all-important for the compound properties. Of particular interest is how the one located at the bicyclooctane ring influences mesomorphic properties.

We have recently synthesized a novel chiral compound from the series of three-ring thiobenzoates, that is (S)-(+)-4-{4-(4-n-pentylbicyclo[2,2,2]octancarbonylthio)benzoyloxy} benzoate 1-methylheptyl, 5boSOMH in short [9]. In this paper we analyze the phase situation in this compound. Its chemical structure is shown in Fig. 2. There are two central bridges in 5boSOMH: a thioester group –COS– (X-bridge) and an ester group –COO– (Y-bridge). Terminal substituents are: an n-pentyl group (R) connected to the bicyclooctane ring and the (S)–(+)–1–methylheptyloxycarbonyl (R′) group at the phenyl ring.

Experimental

The phase polymorphism of 5boSOMH was first established from texture images under a polarizing microscope (Nikon E 200) equipped with a Linkam hot stage (THMSE 600) and temperature controller (TMS 93 Linkam). X-ray measurements were performed by means of a Philips

M. D. Ossowska-Chruściel (✉) · A. Rudzki · J. Chruściel
Institute of Chemistry, University of Podlasie, 3-go Maja 54, 08-110 Siedlce, Poland
e-mail: dch@ap.siedlce.pl

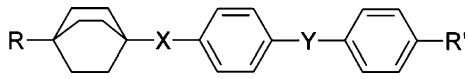

Fig. 1 The chemical structure of mesogens from three rings homologous series

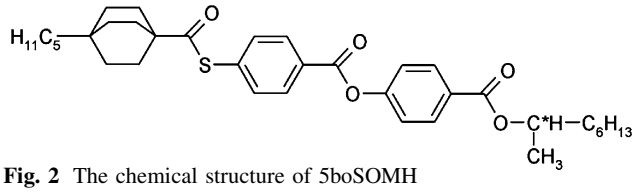

Fig. 2 The chemical structure of 5boSOMH

X'Pert diffractometer and a Guinier symmetrical focusing transmission camera.

The phase transition temperatures as well as changes of enthalpy and entropy upon phase transitions were determined by Differential Scanning Calorimetry (DSC) (Mettler Toledo 822^e), Transmitted Light Intensity (TLI) [10, 11] and by Polarized Light Optical Microscopy (POM).

During the POM and TLI measurments, the sample of 5boSOMH was contained in a Linkam 5 μm cell with the planar orientation and date were collected during heating and cooling with a rate of 2 °C min^{-1}.

Results and discussion

The phase sequence was determined by means of X-ray diffraction. In the SmA* phase the layer spacing d is equal to 33.30 Å, and increases to $d = 34.00$ Å in the SmB* phase. The molecular length l was estimated as the end-to-end distance between the outer hydrogen atoms of the molecule. In the SmA* phase the layer spacing d is approximately 1.12 times the calculated molecular length l (29.65 Å resulting from semiempirical MINDO 3). The angle between the chiral branched terminal chain S-1-methylheptyloxy and the nearest phenyl plane are tilted with respect to each other by c. 90^o in this compound (M.D. Ossowska-Chruściel, M. Cyrański, unpublished data) and other liquid crystals [12, 13]. This result is in good a conformity with crystallographic date, the same as molecular length (M.D. Ossowska-Chruściel, M. Cyrański, unpublished data). This indicates the presence of a smectic structure of the SmA_{1e} subtype. The latter favours dimerization of 5boSOMH much more than does the SmA_1 phase [7]. An influence on the structural B phase is also likely.

DSC curve of 5boSOMH measured between –30 °C and 160 °C with the speed of 2 °C min^{-1} reveals the following transition temperatures: Cr1 (72.8 °C) SmB* (96.0 °C) SmA* (157.4 °C) I. During a cooling cycle, the SmB* phase becomes deeply supercooled down to –30 °C (Cycle A, Fig. 3). An immediately following heating cycle (Cycle B, Fig. 4) reveals two exothermal effects: at 18.3 °C (10.69 kJ mol^{-1}) and 51.4 °C (5.10 kJ mol^{-1}) respectively, see Table 1. Subsequent cooling cycle repeats the observation made during Cycle A (Fig. 3), i.e. SmB* deeply supercooles led to a supercooled smectic B* phase (SmB*), which then during heating forms a metastable crystalline phase Cr2, and then Cr1 (Fig. 4). The latter melts at 71 °C.

The measurements of Transmitted Light Intensity (TLI) were carried out, maintaining the same cooling/heating cycles as during DSC and POM experiments. During the POM and TLI measurements the sample was placed in a Linkam cell.

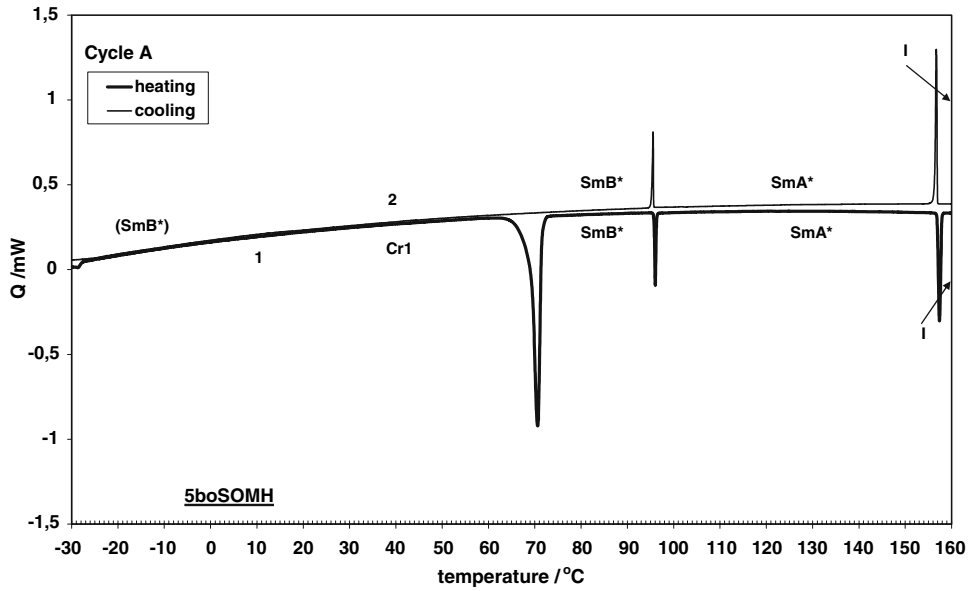

Fig. 3 DSC curve obtained during heating (*curve 1*) and cooling (*curve 2*) of 5boSOMH at the rate of ±2 °C min^{-1}, cycle A

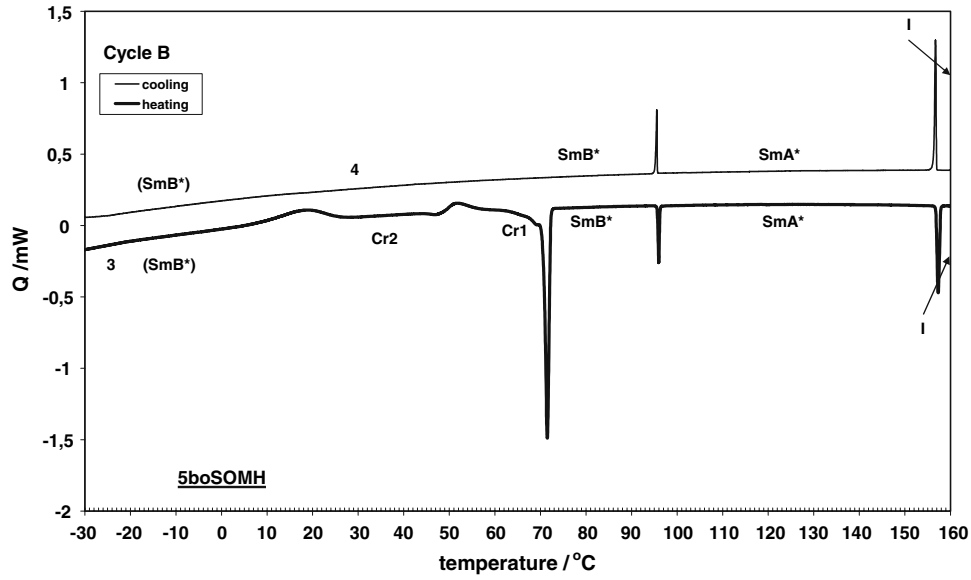

Fig. 4 DSC curve obtained during heating (*curve 3*) and cooling (*curve 4*) of 5boSOMH at the rate of ± 2 °C min^{-1}, cycle B

Table 1 Phase transition temperatures determined by means of TLI, POM and DSC methods and enthalpies (kJ mol^{-1}) of phase transitions for 5boSOMH determined by means of DSC

Cycle	Process	Transition	TLI	POM	DSC	
			T/°C	T/°C ± 0.1	T/°C ± 0.1	ΔH/kJ mol^{-1}
A	Heating	Cr1–SmB*	71.0 ± 0.1	71.5 ± 0.1	72.8 ± 0.1	+27.45 ± 1.05
		SmB*–SmA*	96.0 ± 0.1	96.0 ± 0.1	96.0 ± 0.1	+1.54 ± 0.10
		SmA*–I	160.5 ± 0.1	158.6 ± 0.1	157.4 ± 0.1	+4.20 ± 0.14
	Cooling	I–SmA*	159.1 ± 0.1	157.4 ± 0.1	156.8 ± 0.1	−4.22 ± 0.09
		SmA*–SmB*	96.0 ± 0.1	95.9 ± 0.1	95.7 ± 0.1	−1.52 ± 0.18
B	Heating	(SmB*)–Cr2	17.1 ± 0.1	21.5 ± 0.1	18.3 ± 0.1	−10.69 ± 0.46
		Cr2–Cr1	49.2 ± 0.1	50.0 ± 0.1	51.4 ± 0.1	−5.10 ± 0.24
		Cr1–SmB*	72.7 ± 0.1	71.5 ± 0.1	71.5 ± 0.1	+22.90 ± 0.78
		SmB*–SmA*	96.0 ± 0.1	96.0 ± 0.1	96.0 ± 0.1	+1.52 ± 0.08
		SmA*–I	160.5 ± 0.1	158.7 ± 0.1	157.3 ± 0.1	+4.19 ± 0.12
	Cooling	I–SmA*	159.1 ± 0.1	157.5 ± 0.1	156.8 ± 0.1	−4.20 ± 0.18
		SmA*–SmB*	96.0 ± 0.1	95.9 ± 0.1	95.6 ± 0.1	−1.51 ± 0.18

TLI curve measured during heating (Cycle A) reveals two distinct steps: at 71 °C and 160.5 °C, corresponding to the melting and clearing points, respectively. The SmB*–SmA* transition at 96 °C as a small intensity change shows on the TLI curve. During cooling (Cycle A), the SmA*–SmB* transition at 96 °C is more pronounced than on heating as a clear step in the intensity of transmitted light. Below 96 °C, the TLI curve is smooth and reveals no anomalies down to –30 °C.

Subsequent heating of the supercooled SmB* phase produces a different, more structured TLI curve (Cycle B, Fig. 5, curve 3). At 17.1 °C a well seen increase in transmitted light intensity accompanies the supercooled SmB*—metastable Cr2 transition. The metastable Cr2 phase stays (TLI very slowly, linearly decreases) until the temperature reaches 49.2 °C, at which point it transforms into Cr1, with a clear decrease of TLI. Also the SmB*–SmA* transition is well marked. Thermogram TLI show phase transition SmA^*–I and I–SmA^* very distinctly (Fig. 5).

The textures of orthogonal phases SmB* and SmA* are very similar. A characteristic fan-shaped texture of SmB* transforms into another fan-shaped texture of SmA*, which differs in colour from that of SmB* (Fig. 5). After having completed Cycle B, its texture changes, when the sample is heated. This is characteristic for the development of crystalline phases Cr1 and Cr2, whose textures differ only slightly. We therefore conclude that texture analysis clearly

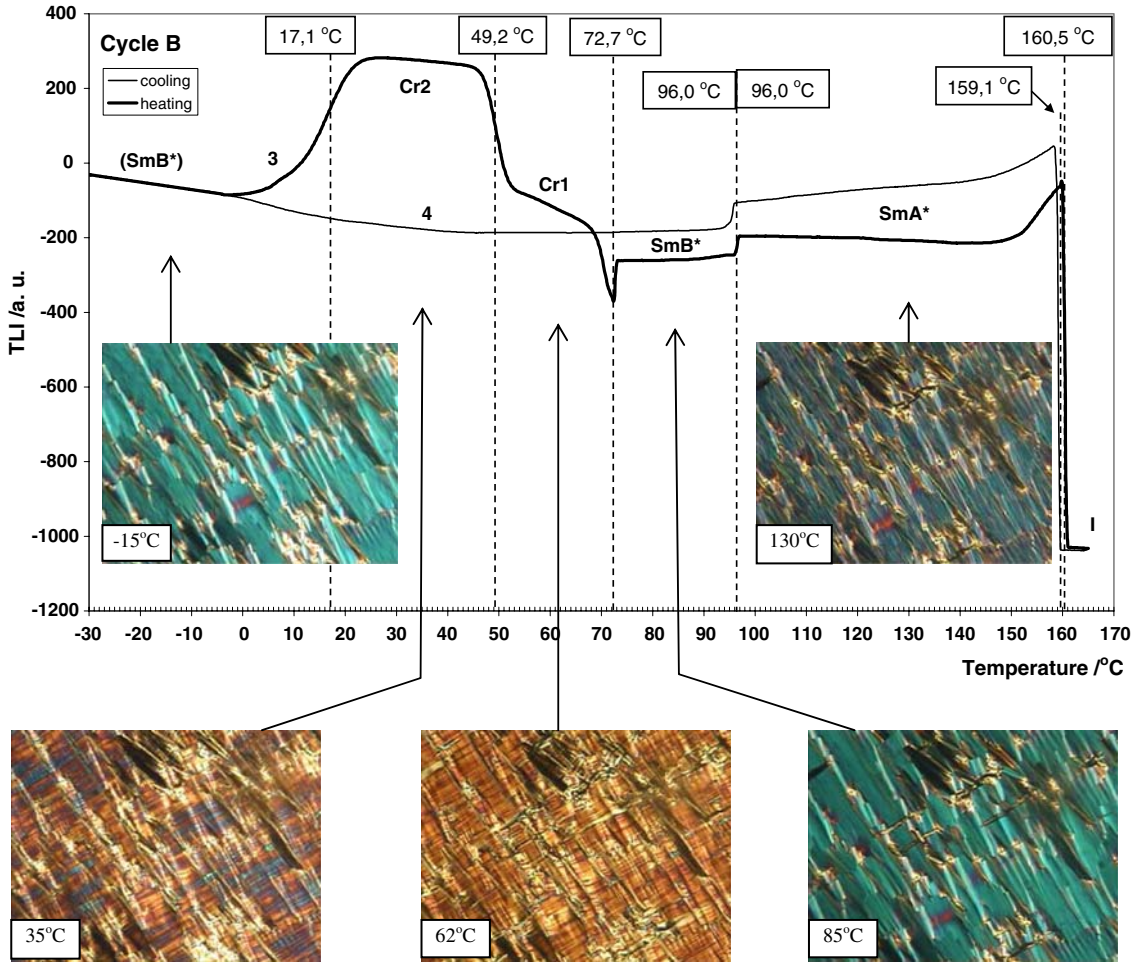

Fig. 5 TLI curves for 5boSOMH for heating (*curve 3*) and cooling (*curve 4*), cycle B

reveals the Cr1–SmB* and SmB*–SmA* phase transitions (Fig. 5). A deep supercooling of the SmB* phase of 5boSOMH was also observed during microscopic texture analysis. No crystallization was detected down to –30 °C (Fig. 5, curve 4).

Phase transition temperatures deduced from DSC, POM and TLI measurements remain in a good agreement. Together with the values of transition enthalpy, they are summarized in Table 1.

Further calorimetric studies were aimed at the analysis of possible influence of the amount of time spent by the 5boSOMH sample at constant temperature upon the Cr2–Cr1 and Cr1-SmB* transition enthalpies. For this purpose, the samples were melted to the SmA* phase (120 °C), then cooled down to 25 °C and kept at that temperature for 1, 5, 6.5, 8, 10, 14, 16, 20 and 24 h. Then, each sample was re-heated to the SmA* phase with the rate of 2 °C min^{-1}. Figure 6 gives the dependence of Cr2–Cr1 and Cr1–SmB* transition enthalpies upon the time spent by the sample at 25 °C.

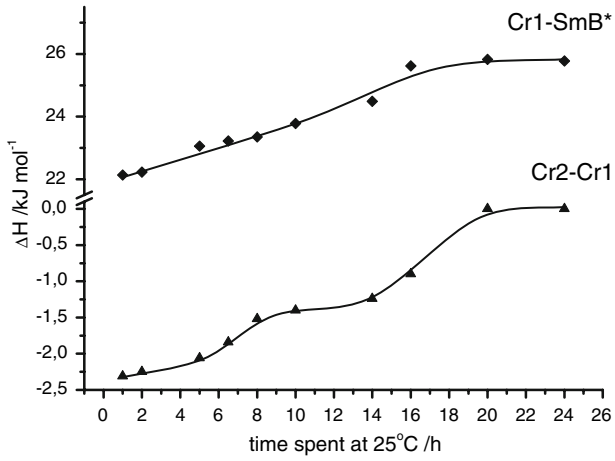

Fig. 6 The dependence of Cr2–Cr1 and Cr1–SmB* transitions enthalpies upon the time spent at 25 °C

It is clear, that the longer the sample stays at 25 °C, the smaller ΔH (Cr2–Cr1) becomes, until it vanishes for 20 hrs waiting time. On the other hand, ΔH (Cr1–SmB*) increases

Table 2 The influence of the cooling rate upon the temperature (°C) and crystallization enthalpy (kJ mol^{-1}) of SmB* phase

Cooling rate (°C min^{-1})	T/°C	ΔH/kJ mol^{-1}
0.1	44.5 ± 0.1	−21.1 ± 0.2
0.2	43.1 ± 0.1	−20.1 ± 0.3
0.5	29.0 ± 0.1	−16.3 ± 0.6
1.0	16.9 ± 0.1	−10.8 ± 0.6
1.5	13.8 ± 0.1	−7.3 ± 0.5
2.0	–	0

with the sample waiting time at 25 °C, and reaches plateau of 25.7 kJ mol^{-1} after 16 h.

Also the influence of the cooling rate upon the temperature and crystallization enthalpy of the SmB* phase was analysed (Table 2). The following cooling rates were used for the analysis: 2 °C min^{-1}, 1.5 °C min^{-1}, 1.0 °C min^{-1}, 0.5 °C min^{-1}, 0.2 °C min^{-1}, 0.1 °C min^{-1}. The results are displayed in Fig. 7 and in Table 2.

The crystallization enthalpy was found to be a linear function of the cooling rate: ΔH = av + b, where a = –10.74, b = 22.11 (Fig. 7). Crystallization temperature also appears to be a function of cooling rate, varying from 44.5 °C for v = 0.1 °C min^{-1} to 13.8 °C for v = 1.5 °C min^{-1}. This is reflected in the existence range of the SmB* phase (Fig. 8).

An interesting property reveals, associated with cooling the sample at v = 2.0 °C min^{-1} from the SmA* phase to either 40 °C or 35 °C in the SmB* phase, and then re-heating it back to SmA* with the same rate. If cooling stops at 40°C then the SmB* phase does not crystallize (there is exothermal transition), and the SmB*–SmA* transition occurs at the same temperature as SmA*–SmB* (Fig. 9a). On the other hand, if the SmB* phase is cooled to

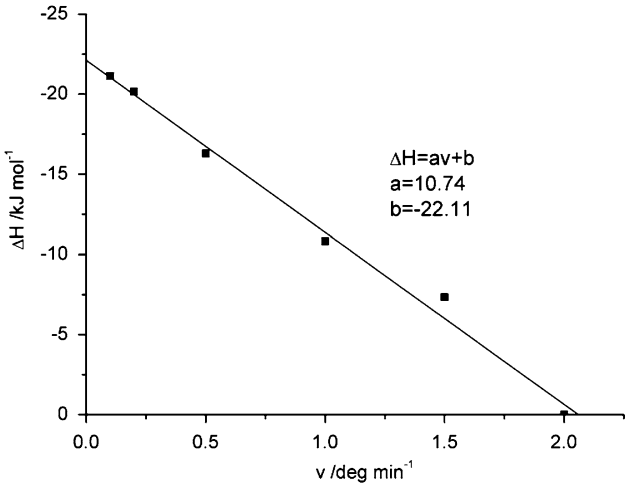

Fig. 7 The crystallization enthalpy as linear function of the cooling rate

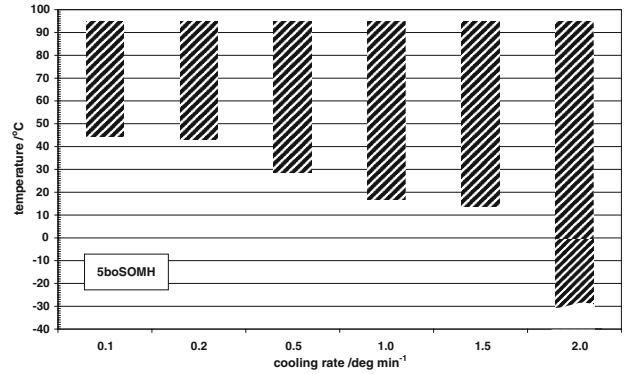

Fig. 8 The existence range of the SmB* phase as function of the cooling rate

35 °C, and then immediately heated up with the same rate of 2.0 °C min^{-1} and then it crystallizes into Cr1. The latter then melts at 71.2 °C again into SmB* (Fig. 9b). It therefore appears that the temperature "turning point" (cooling limit, at which re-heating begins) influences the sample polymorphism during heating. In other words, the 5boSOMH will not crystallize during heating the supercooled SmB* phase if the latter has not been supercooled low enough.

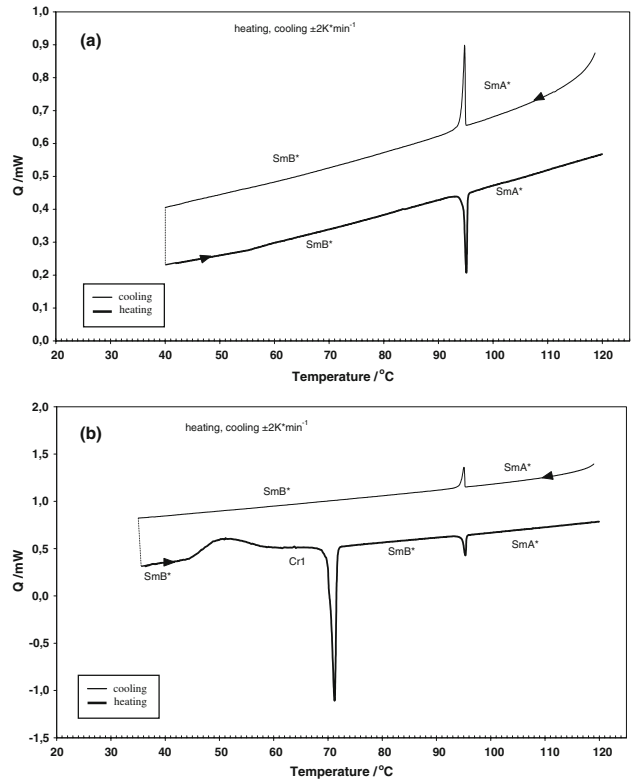

Fig. 9 DSC curves obtained for 5boSOMH during cooling and heating rate ±2 °C min^{-1}: **a** cooling from 120 °C (SmA*) to 40 °C (SmB*) and then re-heating to 120 °C (SmA*); **b** cooling from 120 °C (SmA*) to 35 °C (SmB*) and then re-heating to 120 °C (SmA*)

Conclusions

Although the 5boSOMH has a chiral (S)–(+)–1–methylheptyl terminal substituent in the para position with respect to the central –COO– bridge, it is insensitive to the electrical field in any phase. This compound shows an interesting polymorphism with two enantiotropic liquid crystalline phases SmB* and SmA*. The temperature range of the SmA* is independent of the sample thermal history and, in particular, of the cooling/heating rate. The opposite is true for the SmB* phase of 5boSOMH. SmB* is easily supercooled, and it is up to the cooling rate, how much. If cooled 2.0 °C min^{-1}, the SmB* phase survives down to –30 °C (100 °C supercooling). If cooled 0.1 °C min^{-1}, SmB* crystallizes at 44.5 °C. Heating of the supercooled SmB* phase causes two crystalline phases to develop, whose temperature ranges depend upon the sample thermal history.

The 5boSOMH compound can be considered thermally stable to high degree. The Cr1–SmB* and SmB*–SmA* transitions are well reproduced with repeatable values of thermodynamic parameters, regardless of thermal history of the sample.

Acknowledgement We would like to thank Dr Wojciech Zając for discussions during preparation of the manuscript.

References

1. Apreutesei D, Lisa G, Hurduc N, Scutaru D. Thermal behavior of some cholesteric esters. J Therm Anal Cal. 2006;83:335–40.
2. Demus D, Zaschke H. Flüssige Kristalle in Tabellen II. Leipzig: VEB Deutscher Verlag für Grundstoffindustrie; 1984.
3. Adomenas PV, Nenishkis A, Girdzhyunaite D. Synthesis and mesomorphic properties of aryl-4-(4-alkylbicyclo[2.2.2]octyl) benzoates. Zh Org Khim. 1982;18:812–5.
4. Adomenas PV, Girdziunaite D, Neniskis A, Mazunaitis G. New liquid crystals esters with bicyklo[2,2,2]octane ring. 4th International Liquid Crystal Conference of Socialist Countries, Tbilisi. Abstracts 1981;1:C3.
5. Dąbrowski R, Dziaduszek J, Szulc J, Czupryński K, Sosnowska B. Smectic C compounds with bicyclo[2,2,2]octane ring. Mol Cryst Liq Cyst. 1991;209:201–11.
6. Dąbrowski R, Dziaduszek J, Sosnowska B, Przedmojski J. Ferroelectric liquid crystal materials 4-[2-(4-alkylbicyclo[2,2,2]octyl) ethyl]phenyl 4-alkoxybenzoates, their mesomorphic properties and behaviour in mixtures. Ferroelectrics. 1991;114:229–40.
7. Douglass AG, Czupryński K, Mierzwa M, Kaszyński P. Effects of carborane-containing liquid crystals on the stability of smectic phases. Chem Mater. 1998;10:2399–402.
8. Dąbrowski R, Dziaduszek J, Czupryński K. Synthesis and mesomorphic properties of mesogens containing two ethane or carbonyloxy bridge groups. Proc SPIE. 1995; doi:10.1117/12.215546.
9. Ossowska-Chruściel MD. Synthesis and mesomorphic properties of some new chiral thiobenzoates containing three rings. Liq Cyst. 2007;34:195–211.
10. Ossowska-Chruściel MD, Zalewski S, Rudzki A, Feliks A, Chruściel J. The phase behaviour of 4-n-pentylphenyl-4'-n-heptyloxythiobenzoate. Phase Transitions. 2006;79:679–90.
11. Chruściel J, Zalewski S, Ossowska-Chruściel MD, Filiks A, Rudzki A. Transmisyjne metody optyczne. In: Mikuli E, Migdał-Mikuli A, editors. Komplementarne metody badań przemian fazowych (in polish). Jagiellonian University, Kraków; 2006. p. 247–70.
12. Hori K, Kawahara S, Ito K. Crystal structures of antiferroelectric mesogen, 4-[(s)-1-methylpentyloxycarbonyl]phenyl 4'-octyloxybiphenyl-4-carboxylate and ferroelectric mesogen, 4-[(s)-1-methylhexyloxycarbonyl]phenyl 4'-octyloxybiphenyl-4-carboxylate. Ferroelectrics. 1993;147:91–4.
13. Hori K, Endo K. Crystal structure and polymorphism of antiferroelectric mesogen, 4-[(S)-1-methylheptyloxycarbonyl]phenyl 4′-Octyloxybiphenyl-4-carboxylate (MHPOBC). Bull Chem Soc Jpn. 1993;66:46–50.